



ORNL/Sub-21453/2

cy. 24

F

3 1980

60 GHz and 110 GHz DEVELOPMENT PROGRAM

**J. Shively, C. Conner, H. Jory, D. Stone,
R. Symons, G. Thomas, G. Wendell**

**Quarterly Report No. 2
October through December 1979**

FUSION ENERGY DIVISION LIBRARY

Prepared for:

**Oak Ridge National Laboratory
Oak Ridge, Tennessee 37830**

Operated by:

**Union Carbide Corporation for the Department of Energy
Contract No. W-7405-eng-26**

Varian Associates, Inc.
Palo Alto Microwave Tube Division
611 Hansen Way
Palo Alto, California 94303

This report was prepared as an account of work sponsored by an agency of the United States Government. Neither the United States Government nor any agency thereof, nor any of their employees, contractors, subcontractors, or their employees, makes any warranty, express or implied, nor assumes any legal liability or responsibility for any third party's use or the results of such use of any information, apparatus, product or process disclosed in this report, nor represents that its use by such third party would not infringe privately owned rights.

60 GHz and 110 GHz DEVELOPMENT PROGRAM

J. Shively, C. Conner, H. Jory, D. Stone,
R. Symons, G. Thomas, G. Wendell

Quarterly Report No. 2
October through December 1979

Prepared for:
Oak Ridge National Laboratory
Oak Ridge, Tennessee 37830

Operated by:
Union Carbide Corporation for the Department of Energy
Contract No. W-7405-eng-26

Varian Associates, Inc.
Palo Alto Microwave Tube Division
611 Hansen Way
Palo Alto, California 94303

TABLE OF CONTENTS

<u>Section</u>		<u>Page</u>
I.	INTRODUCTION	1
II.	60 GHz 200 kW PEAK OSCILLATOR	3
	A. Electron Gun Computer Design	3
	B. Superconducting Solenoid Magnet Computer Design	3
	C. Interaction Circuit	3
	D. Output Window	11
III.	110 GHz 200 kW CW OSCILLATOR	12
	A. Electron Gun Computer Design	12
	B. Interaction Circuit	17
	C. Output Window	25
IV.	WATERLOADS, POWER SAMPLERS AND ARC DETECTORS	26
V.	PROGRAM SCHEDULE AND PLANS	27
VI.	REFERENCES	33

LIST OF ILLUSTRATIONS

<u>Figure</u>		<u>Page</u>
1.	60 GHz Gun Trajectory Plot	4
2.	Transverse Energy Profile of Preliminary 60 GHz Gun Design	5
3.	Anode	6
4.	Normalized Pumping Speed vs Normalized Channel Diameter at Fixed RF Isolation	9
5.	Mode Density	10
6.	Transverse Energy Profile for the Best 25° Cathode Design	13
7.	110 GHz Gun Trajectory Plot	14
8.	Transverse Energy Profile as a Function of 1st Anode Voltage	15
9.	Variation of Transverse Energy Profile with 1st Anode Angle (Curved Back Focus Electrode)	16
10.	Transverse Energy Profile as a Function of Bucking Coil Ampere-Turns	18
11.	Beam Radius at Circuit as a Function of Change in Bucking Coil Ampere-Turns	19
12.	Transverse Energy Profile as a Function of Distance From Center of Cathode to Tip of First Anode	20
13.	Variation of Transverse Energy Profile with Beam Current	21
14.	Transmission of TE ₁₁ Mode through Anode Load vs Load Gap and Frequency	22
15.	Effective Interaction Cavity Length	24
16.	Milestone Chart	28

ABSTRACT

The objective of this program has been changed from developing a microwave amplifier or oscillator capable of producing 200 kW CW power output at 110 GHz to developing families of microwave oscillators capable of producing 200 kW of peak power output at 60 GHz and some higher frequency, possibly 90 GHz or 110 GHz, with pulse durations at 100 ms, 30 s and CW. The use of cyclotron resonance interaction is being pursued.

The early design phases of this program are discussed.

I. INTRODUCTION

The objective of this program has been changed from developing a microwave amplifier or oscillator capable of producing 200 kW of CW power at 110 GHz to developing families of microwave oscillators capable of producing 200 kW of peak power output at 60 GHz and some higher frequency, possibly 90 GHz or 110 GHz, with pulse durations at 100 ms, 30 s and CW. Tunability or bandwidth is not considered an important parameter in the design, but efficiency is. Mode purity in the output waveguide is not a requirement for the device, but the circular electric mode is considered desirable because of its low loss properties.

With these objectives in mind, an approach based on cyclotron resonance interaction between an electron beam and microwave fields is being pursued. The detailed arguments leading to this approach are contained in the final report of a preceding study program.¹ The device configurations of particular interest, called gyrotrons, have been discussed in recent literature.²⁻⁵ They employ a hollow electron beam interacting with cylindrical resonators of the TE_{om1} class.

The optimum beam for the cyclotron resonance interaction is one in which the electrons have most of their energy in velocities perpendicular to the axial magnetic field. Another requirement is that the spread in the axial components of the electron velocities be as small as possible. Electrons which have different axial velocities will not interact efficiently.

The approach chosen to generate the beam is a magnetron type of gun as is used on the 28 GHz gyrotron, also developed for Oak Ridge National Laboratory.^{6,7} With this type of gun the shaping of the magnetic field in the gun region becomes quite important.

The 60 GHz gyrotron development is progressing on schedule. The $3A/cm^2$ gun design is nearing completion. The superconducting solenoid magnet design is nearly complete. Techniques for loading the anode drift tube are being investigated. Overcoming the pumping impedance at the small beam

tunnel is being explored. Cold test models are being fabricated and cold test components are on order. The microwave design of the window is complete and ceramics are on order.

The 110 GHz gyrotron development has been terminated. Prior to termination the electron gun computer design was completed and mechanical design started. A drift tube load cavity had been designed. Cold test measurements directed at determining the effective interaction cavity length were completed. A variety of output/collector coupling schemes were considered. A window was designed and ceramics received. Piece parts for the waterload, power sampler and arc detector were received.

II. 60 GHz 200 kW PEAK OSCILLATOR

A. ELECTRON GUN COMPUTER DESIGN

The 60 GHz gun design has a mean cathode radius of 0.175". The cathode loading is 3 A/cm². A plot of nine trajectories is shown in Figure 1.

Figure 2 shows the transverse energy profile for the 60 GHz gun design whose trajectories were plotted in Figure 1. The transverse velocity variation of this design is $\pm 3.25\%$. The design calls for a curved back focus electrode.

Additional work will be done to see if the curved back focus electrode can be replaced by a straight (conical) one.

B. SUPERCONDUCTING SOLENOID MAGNET COMPUTER DESIGN

Since it is desired to increase the bucking coil radius in order to achieve better voltage holdoff characteristics, additional runs will be made to verify that a satisfactory transverse energy profile can be obtained with the larger radius.

A new Varian magnetostatic program has now become available which computes the normalized flux array for an iron-free magnet system in a form suitable for use in the gun program. Both on-axis and off-axis axial and radial components of flux density are computed as well as the vector potential. This new program is in the final stage of debugging and will be used for future computations on this project.

C. INTERACTION CIRCUIT

1. Anode Design - Beam Tunnel

The beam tunnel design is sketched in Figure 3. This assembly is composed of the second anode electrode face on one end and the load cavity on the other end. Following the adiabatic compression of the electron beam,

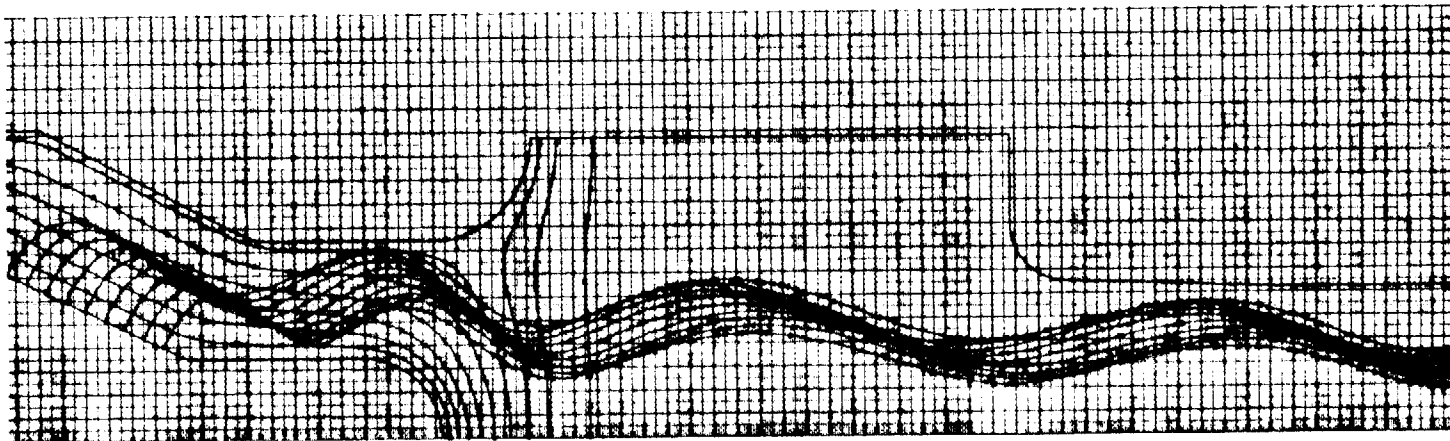


FIGURE 1. 60 GHz GUN TRAJECTORY PLOT

WEIGHTED MEAN TRANSVERSE ENERGY $\mu = 65,226$ keV

WEIGHTED STANDARD DEVIATION OF TRANSVERSE ENERGY $\sigma = 4,265$ keV (6.5%)
TRANSVERSE VELOCITY VARIATION = $\pm 3.25\%$

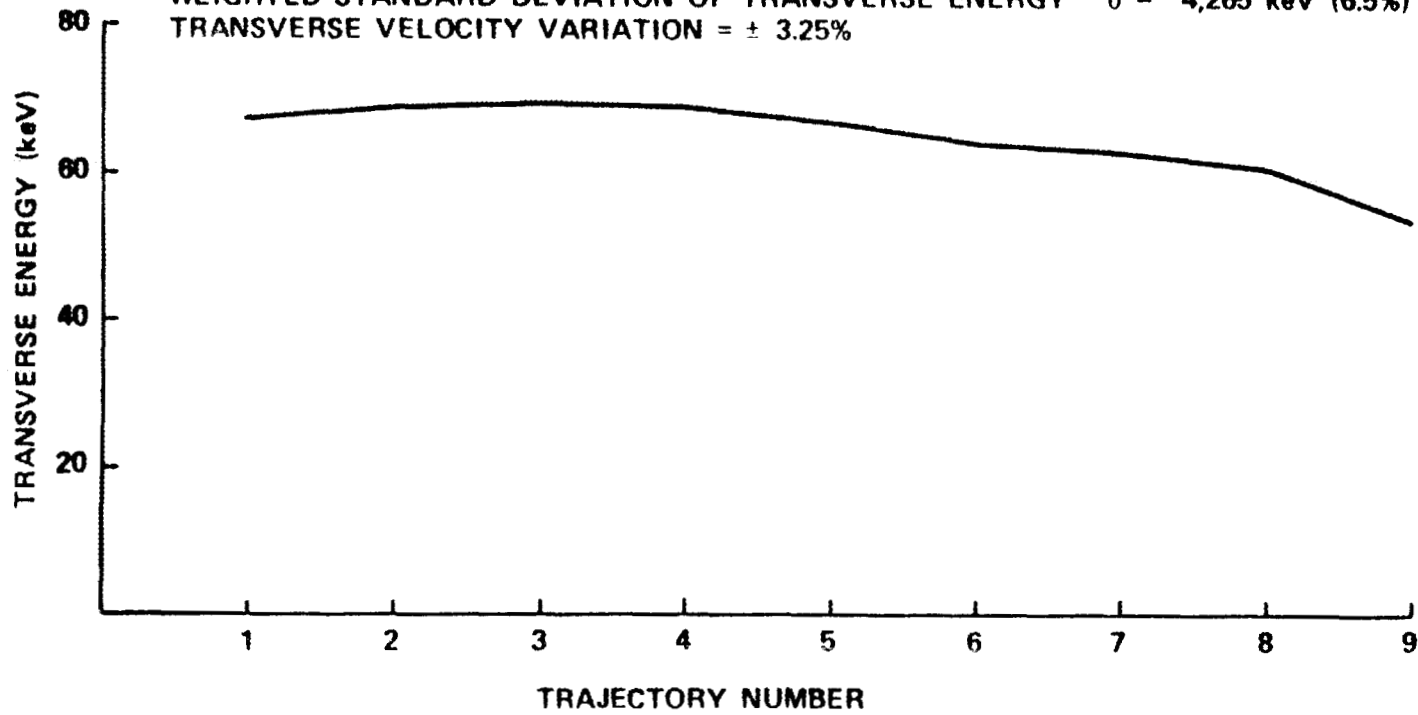


FIGURE 2. TRANSVERSE ENERGY PROFILE OF PRELIMINARY 60 GHz GUN DESIGN

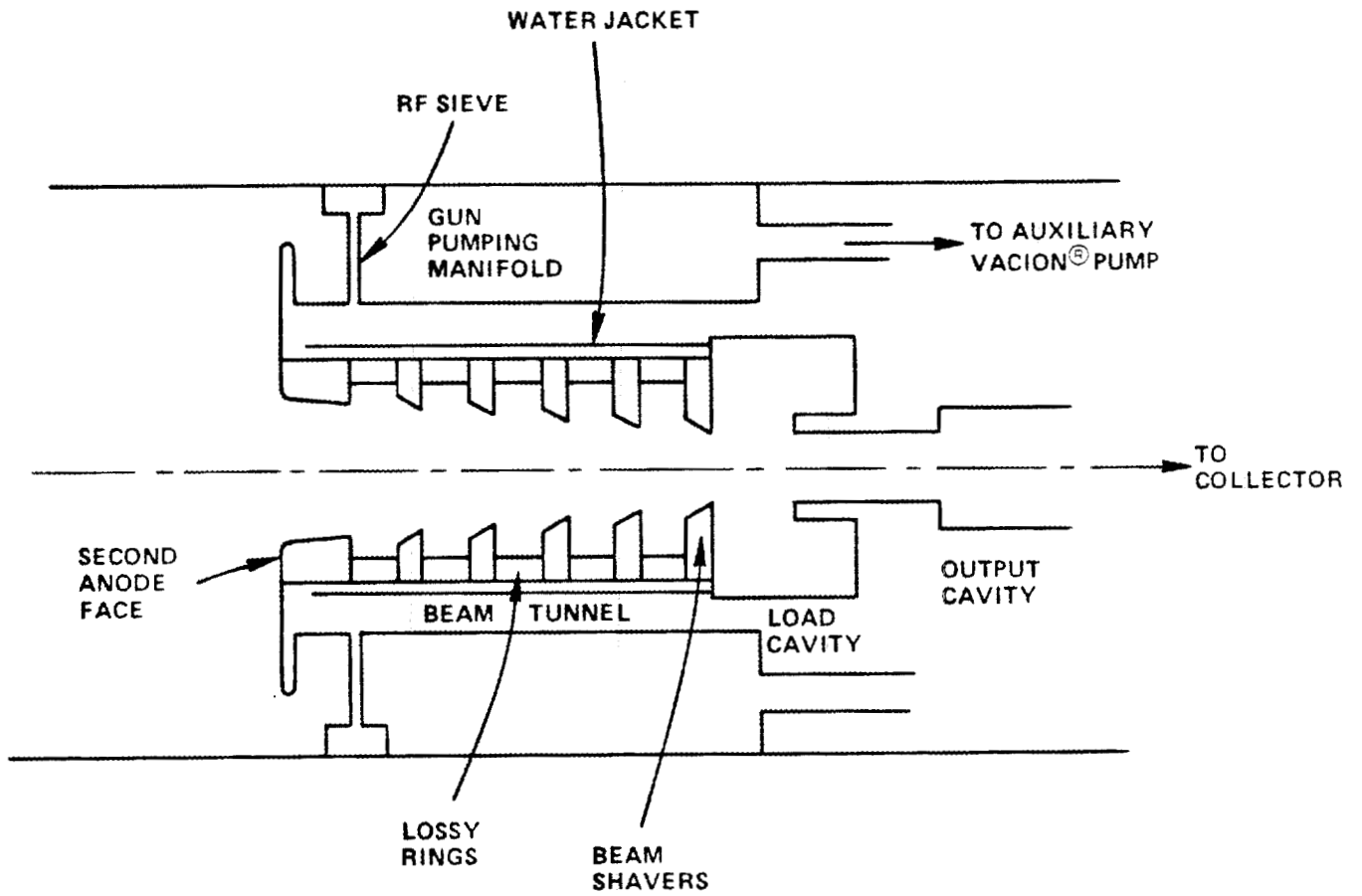


Figure 3. ANODE

the beam tunnel contracts in diameter as it runs toward the interaction circuit. In order to prevent parasitic oscillations in the beam tunnel, this region has been designed for high rf loss. Carberlox loss rings, alternated with metal beam shaving rings, provide an axisymmetric loss structure. The carberlox rings are recessed, with a larger inner diameter than the beam shaving rings to prevent electrostatic charging by stray electrons. To avoid any cylindrical structure which is capable of exciting oscillations, the individual metal beam shavers have conically tapered beam holes. At critical locations such as the anode face and the entrance to the load cavity, the shavers will be made of molybdenum to reduce sputtering damage in case of beam interception. Enclosed in a copper sleeve, the entire beam tunnel assembly will be housed in a water jacket. Ceramic parts for the beam tunnel are on order and mechanical design of the assembly is in progress.

2. Anode Design - Gun Pumping Manifold

In order to avoid cathode poisoning during gas bursts in the tube, it is necessary to provide sufficient (≈ 1 L/sec) pumping speed at the gun. Unfortunately, because of space restrictions, the gyrotron VacIon^R pumps must be located at the collector end of the tube and the beam tunnel is then used as the pumping path to the gun. The addition of a separate gun pumping manifold has become necessary in high frequency gyrotrons because, as the beam tunnel diameter is reduced, the pumping speed of the beam tunnel pumping path drops sharply as shown in Table I.

TABLE I
Pumping Speed

Device	Freq. (Ghz)	Pumping Speed (l/s)
VGA-8000	28	3.0
VGE-8060	60	0.4
VGT-8010	110	0.05

The gun pumping manifold will surround the beam tunnel assembly and terminate near the face of the second anode. A separate 8 L/sec VacIon pump

will connect into the pumping manifold via a long pumping line which runs toward the collector end of the tube.

Past experience has shown that it is necessary to baffle the gun end of the gun pumping manifold with an rf sieve in order to avoid rf heating of the auxiliary VacIon pump. The sieve must attenuate rf without cutting down on the pumping speed. Assuming that the sieve will contain a large number of long, circular cross-section holes, the optimum hole size for good pumping speed, combined with good rf attenuation, lies in a narrow range, as shown in Figure 4. With a suitable sieve design, the gun pumping system should provide a total pumping speed of ~ 2 L/sec at the gun. Mechanical design of the pumping manifold is proceeding.

3. Cavity Design

Cold test cavities for the 60 GHz oscillator have been fabricated. The TE_{02} cavity, when properly loaded, has an external Q of 520 ± 50 . Further cold tests are in progress on the TE_{02} and TE_{03} cavities.

Experience with the 28 GHz oscillator indicates that modes other than the desired cavity mode may compete for interaction with the electron beam. Particularly troublesome are modes with the same radial mode number and roughly the same frequency as the desired mode. The competing mode densities of a 60 GHz TE_{01} and a 60 GHz TE_{02} oscillator are compared in Figure 5. Sister modes of the TE_{011} and TE_{021} with axial mode numbers greater than unity, and all other modes with axial mode numbers greater than six, have been omitted for clarity. The TE_{22p} family of modes have proven to be troublesome in the 28 GHz devices which operate in the TE_{021} cavity mode. The TE_{32p} family of modes may also have been observed in mode competition in these devices, but are too far removed from the TE_{021} in frequency to cause significant problems.

As shown in Figure 5, a TE_{011} oscillator would be subject to a far lower competing mode density than a TE_{021} device, although the TE_{216} and the TE_{311} may give difficulties. For this reason, we are exploring the possibility of using the TE_{011} cavity mode for the 60 GHz oscillator. A

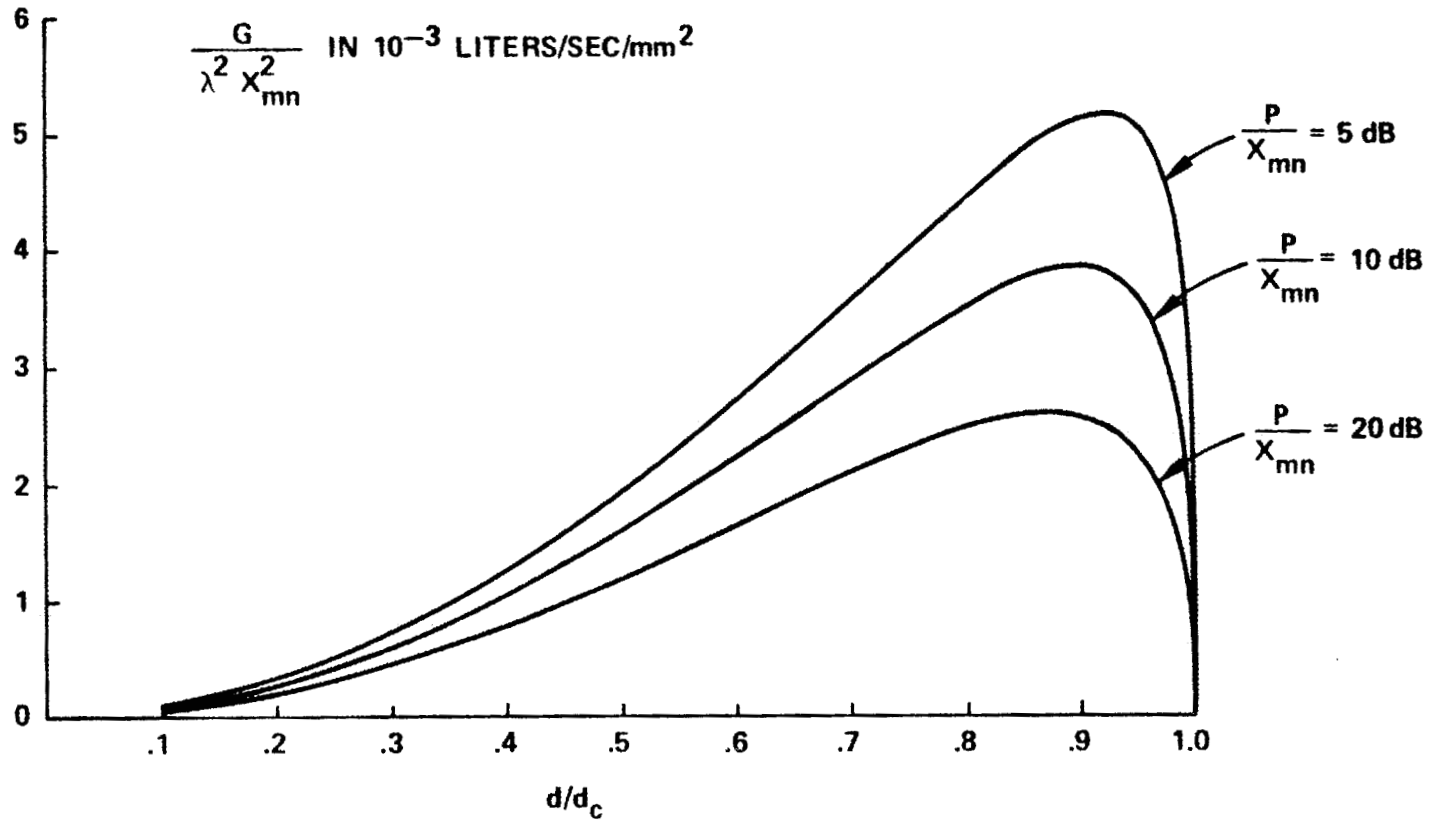


FIGURE 4. NORMALIZED PUMPING SPEED vs NORMALIZED CHANNEL DIAMETER AT FIXED R.F. ISOLATION

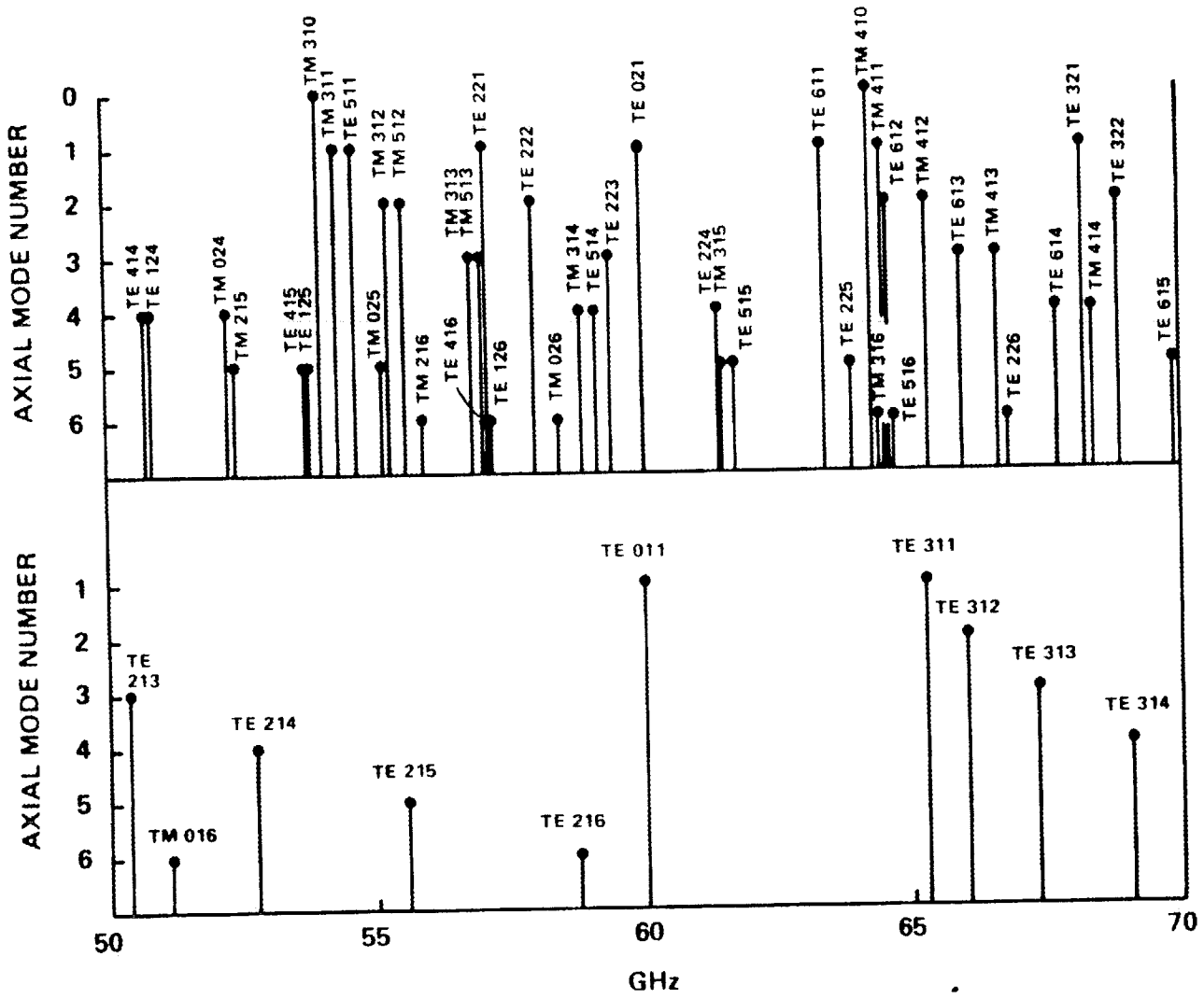


Figure 5. MODE DENSITY

TE₀₁ 60 GHz cold test cavity has been made and cold testing is proceeding. Other means of suppressing mode competition are under investigation.

D. Output Window

During the report period the electrical design of the output window was completed. For CW operation, a double disc window with face cooling (FC75) was designed with a .050" FC75 gap using both AL-995 and BeO (99.5%) ceramics. A computer program was written and used to determine the ceramic thicknesses needed for a match at 60 GHz. These values are .524 λ g for AL-995 and .529 λ g for BeO (99.5%). In terms of actual dimensions, these translate to .0413" and .0338", respectively. To insure that the ceramic can withstand stress due to heating and pressure, BeO ceramics with thicknesses of 1.529 λ g (0.120") and 2.529 λ g (0.198") and AL-995 ceramics with thicknesses of 1.524 λ g (0.099") and 2.524 λ g (0.163") were ordered. Delivery is expected by March 1, 1980.

A single disc BeO window was designed for the experimental pulsed oscillators. To insure mechanical integrity, the window thickness was chosen as 1.5 λ g or 0.117". Ceramics were ordered and delivery is expected by March 1, 1980.

Mechanical design is started and will be completed during the next quarter.

III. 110 GHz 200 kW CW OSCILLATOR

A. Electron Gun Computer Design

Since 3 A/cm^2 cathode loading could only be achieved at a 0.168" mean cathode radius by using a compound curvature of the cathode surface rather than a conical surface, it was, for ease of construction, decided to use a loading of 4 A/cm^2 for the 110 GHz gun design.

Various designs using a 25° cathode angle instead of 23° were tried on the computer with good results. The transverse energy profile for the best 25° design is shown in Figure 6. The transverse velocity variation at the interaction circuit for this case is $\pm 2.45\%$. Nine trajectories were used in the computer simulation. Figure 7 is the plot of these trajectories as computed by the XGUN program.

A number of computer runs were made using this design in order to determine the sensitivity of the transverse energy profile to various parameter variations.

The first anode voltage for this design is 15,800 volts. Two additional computer runs were made--one at 15,500 volts and one at 16,100 volts. The resulting transverse energy profiles are shown in Figure 8.

To determine the effect of changing the angle of the first anode, five computer runs were made with the following angles:

1. 25.590°
2. 26.362°
3. 27.604°
4. 28.724°
5. 29.930°

The results of the runs are plotted in Figure 9. In this case eight trajectories were used and the graph shows the transverse energy at the interaction circuit for each trajectory and each first anode angle.

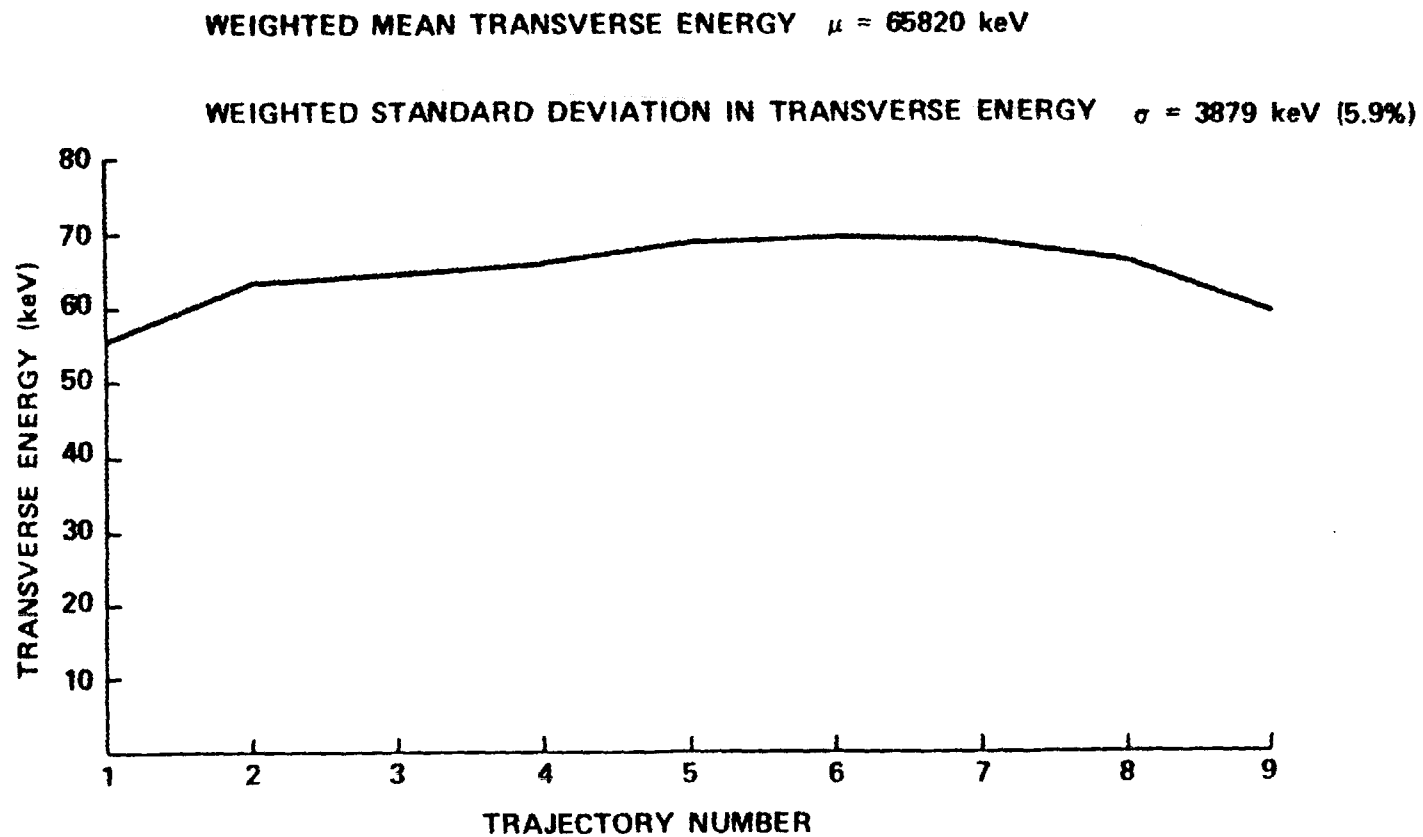


FIGURE 6. TRANSVERSE ENERGY PROFILE FOR THE BEST 25° CATHODE DESIGN

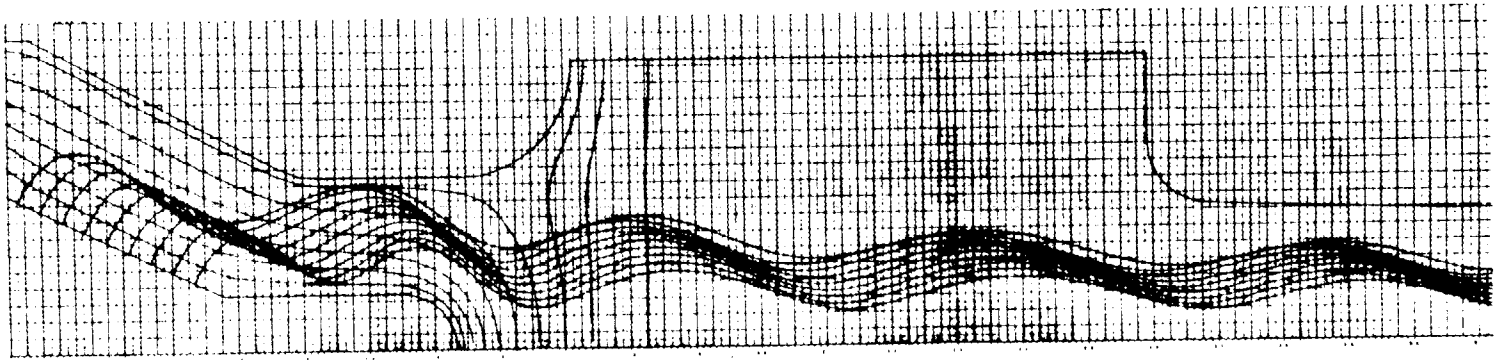


FIGURE 7. 110 GHz GUN TRAJECTORY PLOT

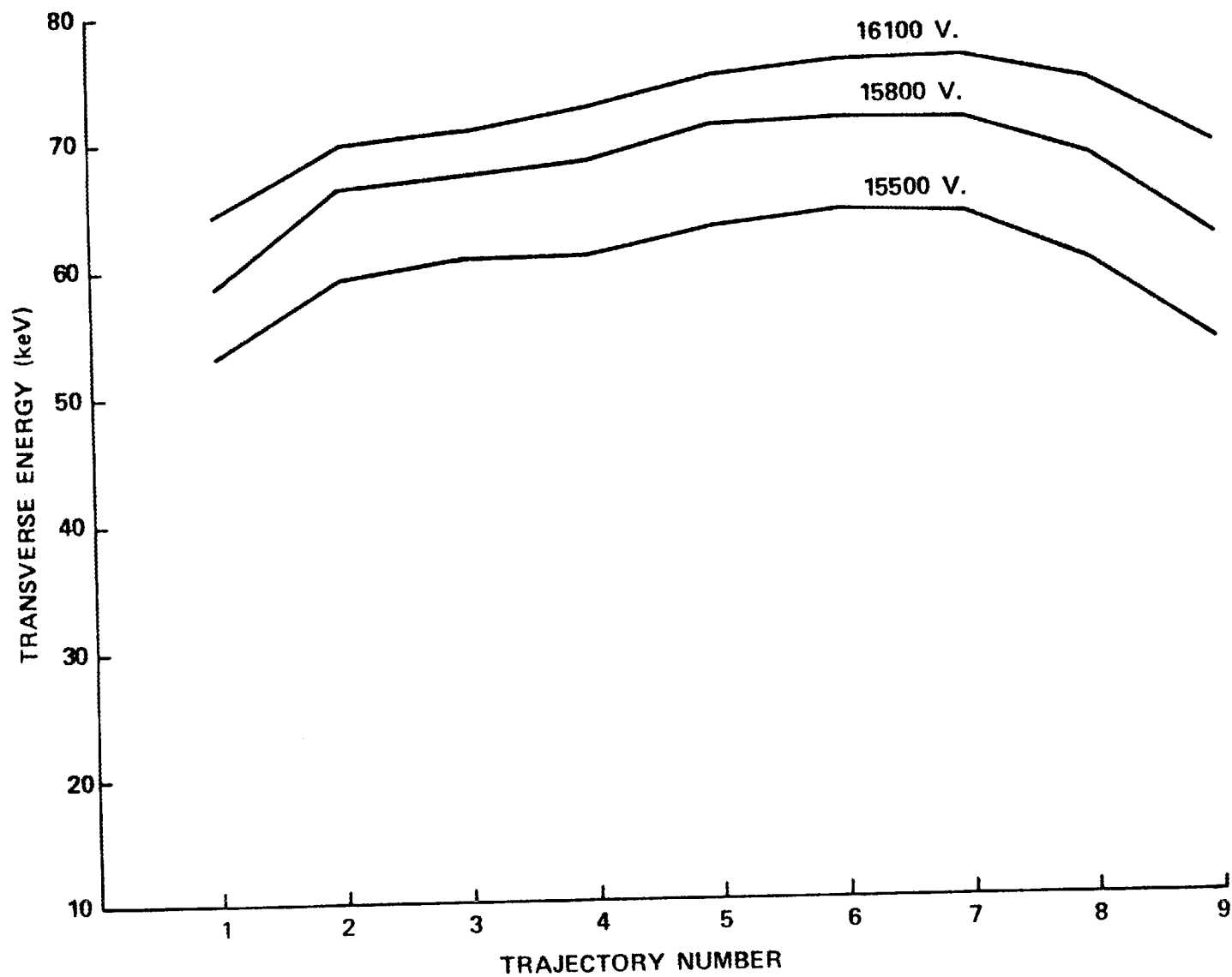


FIGURE 8. TRANSVERSE ENERGY PROFILE AS A FUNCTION OF 1ST ANODE VOLTAGE

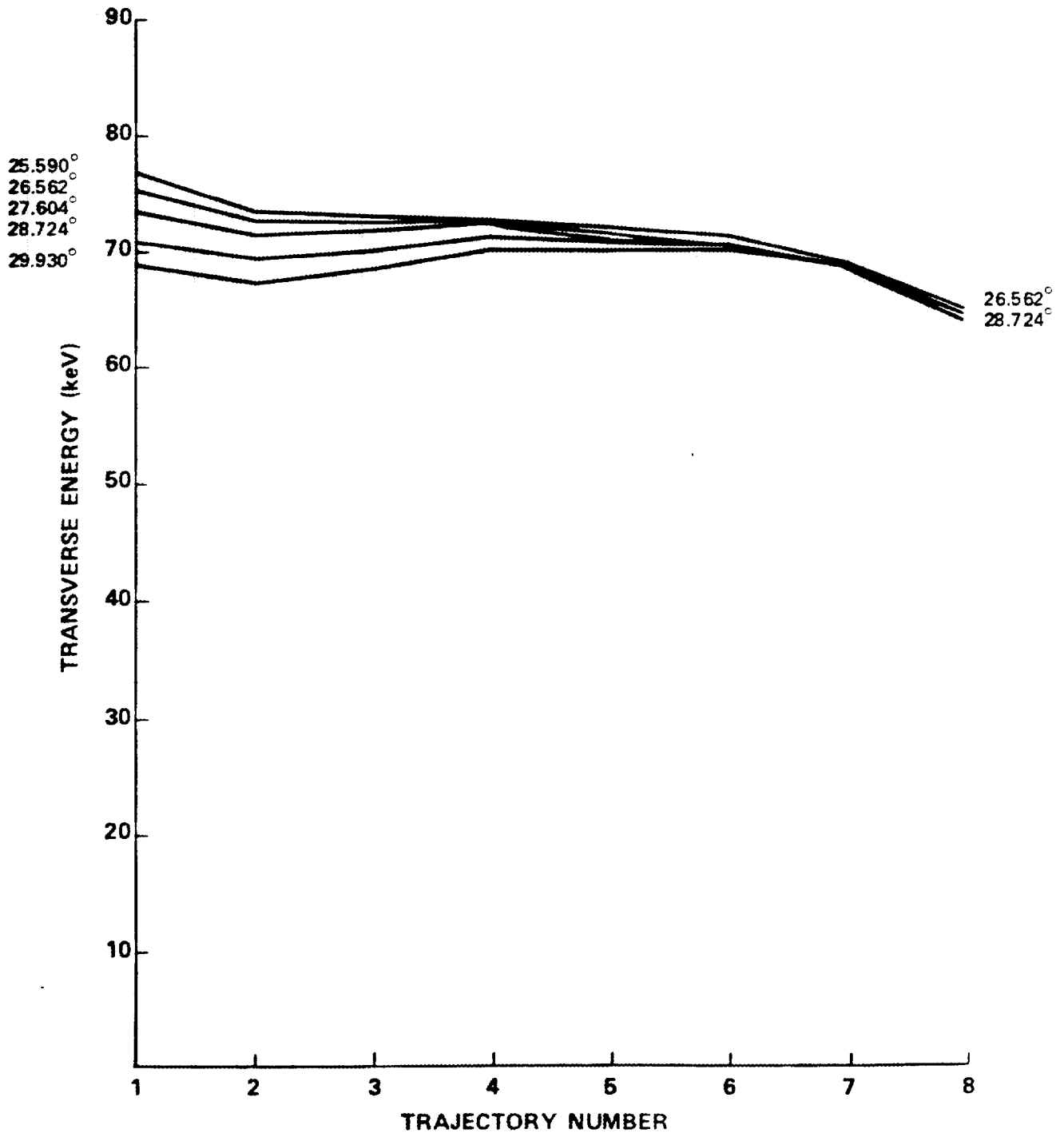


FIGURE 9. VARIATION OF TRANSVERSE ENERGY PROFILE WITH 1ST ANODE ANGLE (CURVED BACK FOCUS ELECTRODE)

Since the current in the bucking coil at the cathode will probably be adjusted for trimming purposes, it seemed desirable to determine the sensitivity of the gun performance to nominal changes in this current. Two additional runs were made by recomputing the input magnetic field profiles for changes in the bucking coil current of -10% and -20%. The effects of these changes on the transverse energy profile are seen in Figure 10. Raising the current in the bucking coil is tantamount to lowering the field at the cathode. This has the same effect as raising the voltage at the first anode.

From these same runs it was possible to determine the beam radii at the interaction circuit for each of the three cases, assuming adiabatic compression. A graph of these results can be seen in Figure 11.

Figure 12 shows the results of small perturbations in the distance from the center of the cathode to the tip of the first anode.

The nominal beam current is 8 amperes. Since there may be occasions when different beam currents may be used, the effect of changing the beam current on the transverse energy profile was investigated. Three runs were made on another similar design at 5 A/cm^2 loading. The effects are shown in Figure 13.

B. Interaction Circuit

1. Load Cavity Design

We have measured the transmission loss of TE_{11} radiation launched at the oscillator cavity drift tube, through the load cavity designed for the 110 GHz oscillator. The loss element in the load cavity is a water-cooled lossy ceramic rather than a water-backed ceramic window as has been used in the 28 GHz designs. The advantage of this approach is that it makes the load cavity more broadband. The load cavity transmission fraction is plotted versus frequency for various load cavity drift tube gap sizes in Figure 14. At larger gap sizes the loss becomes less sensitive to

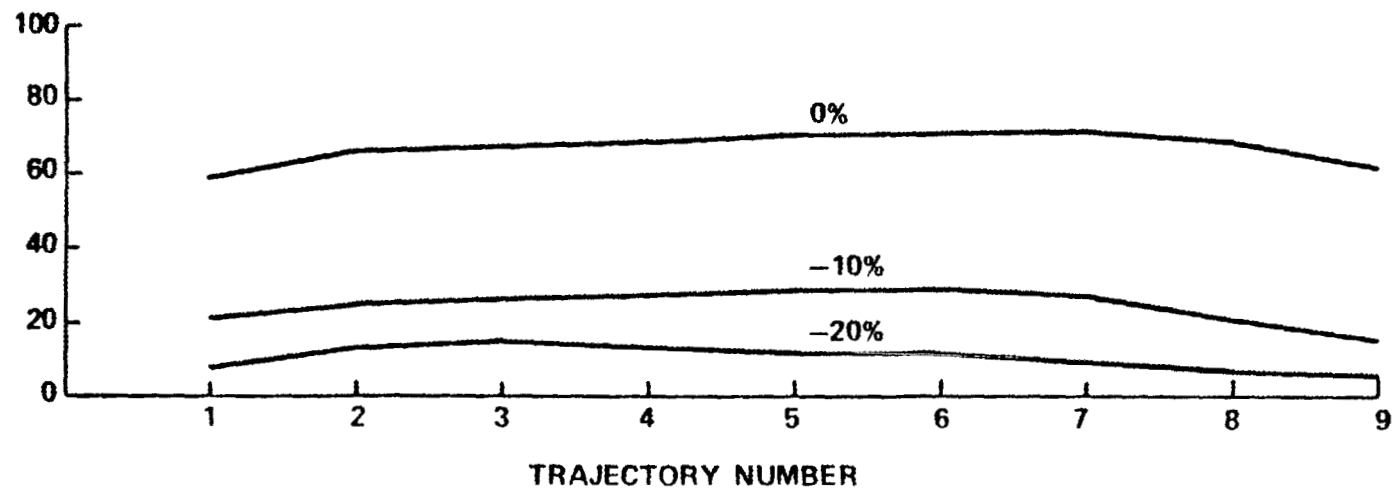


FIGURE 10. TRANSVERSE ENERGY PROFILE AS A FUNCTION OF BUCKING COIL AMPERE-TURNS

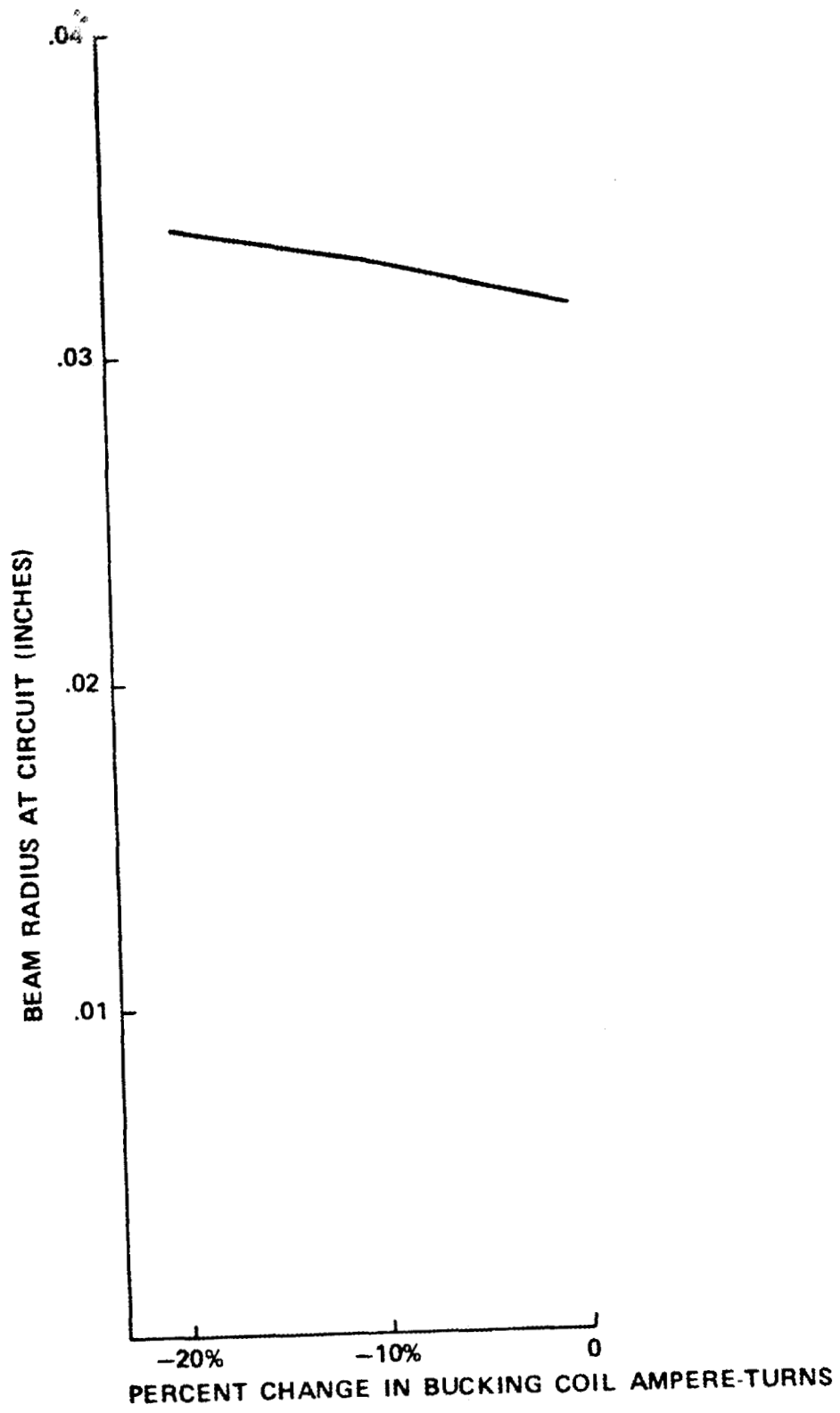


FIGURE 11. BEAM RADIUS AT CIRCUIT AS A FUNCTION OF CHANGE IN BUCKING COIL AMPERE-TURNS

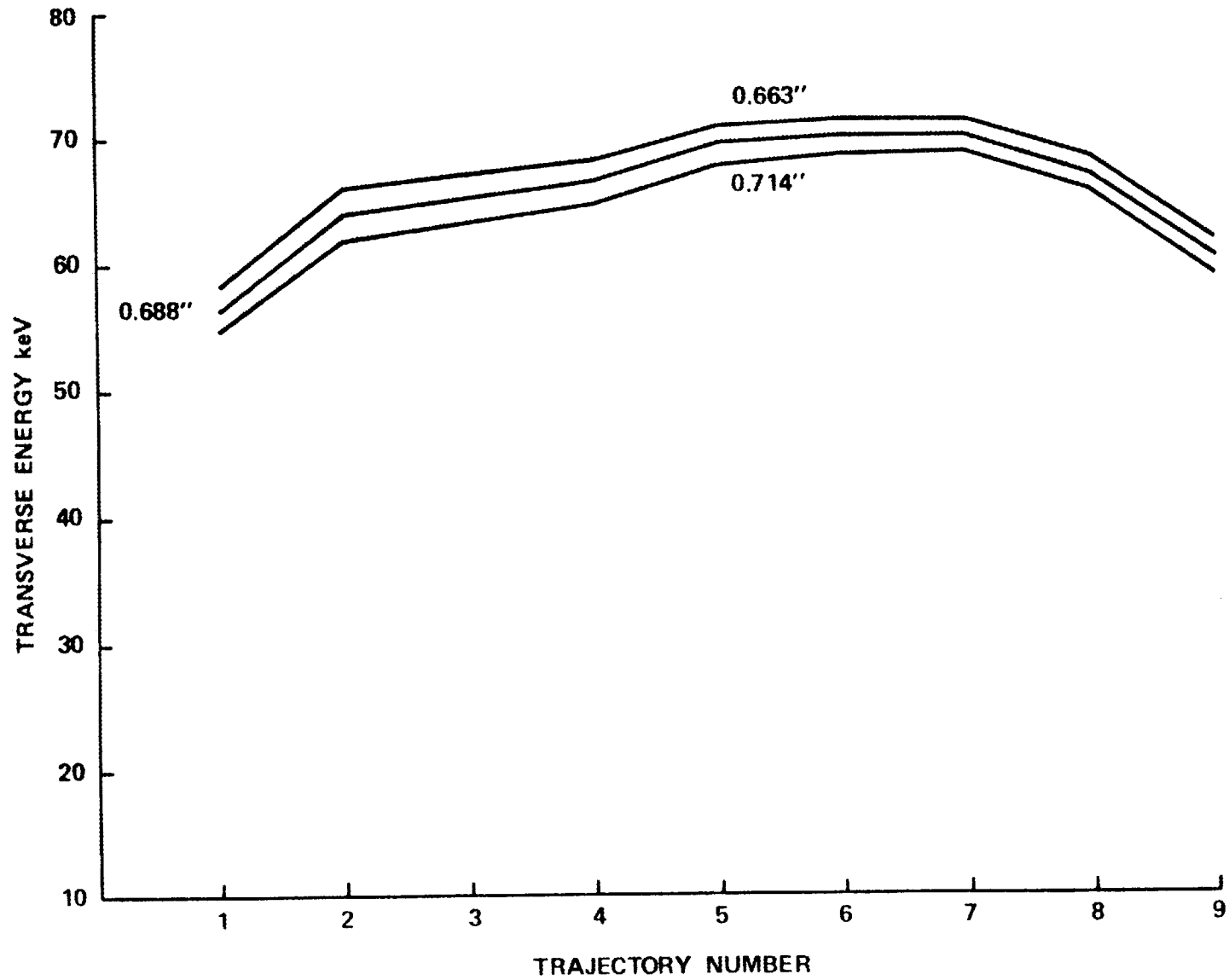


FIGURE 12. TRANSVERSE ENERGY PROFILE AS A FUNCTION OF DISTANCE FROM CENTER OF CATHODE TO TIP OF FIRST ANODE

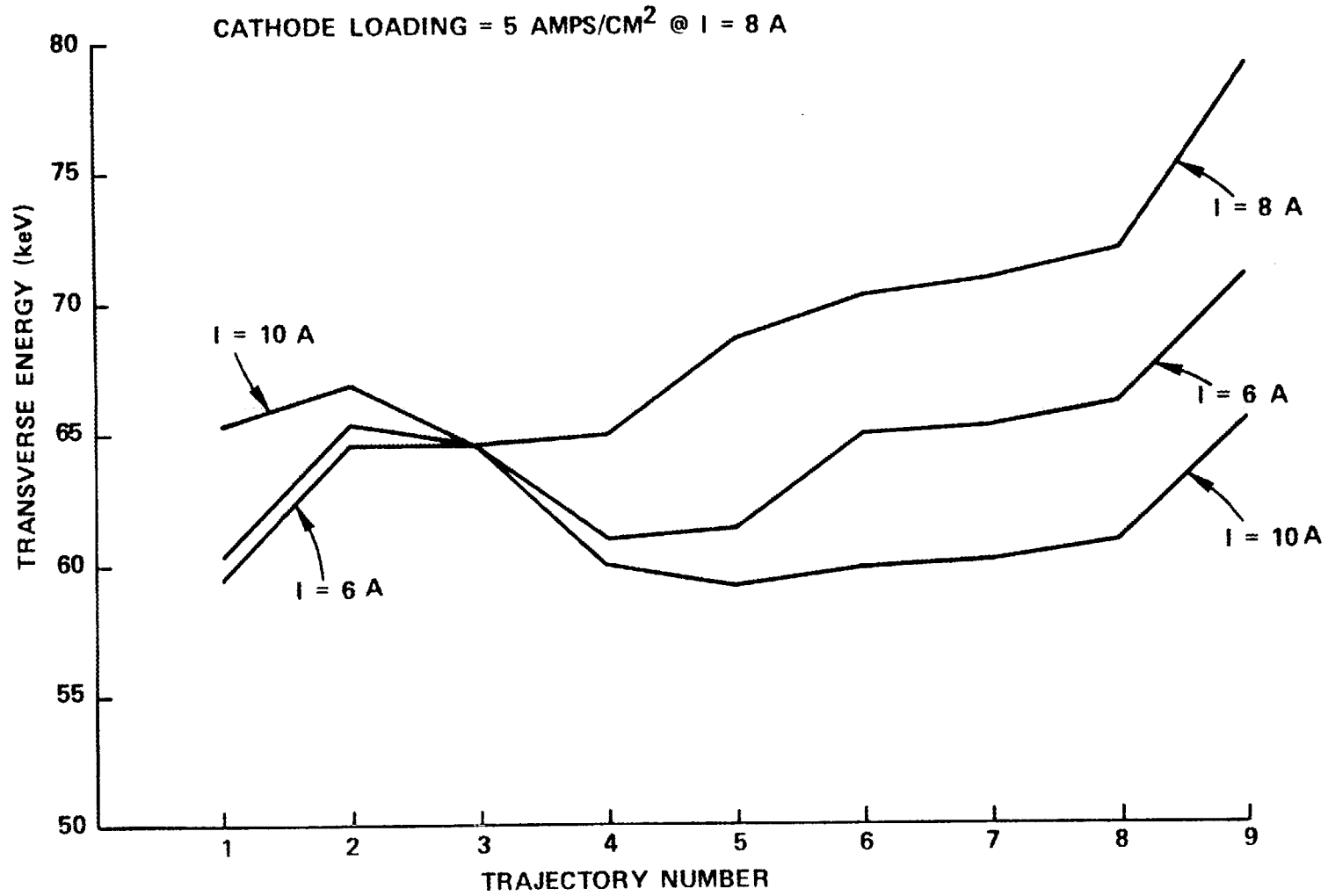


FIGURE 13. VARIATION OF TRANSVERSE ENERGY PROFILE WITH BEAM CURRENT

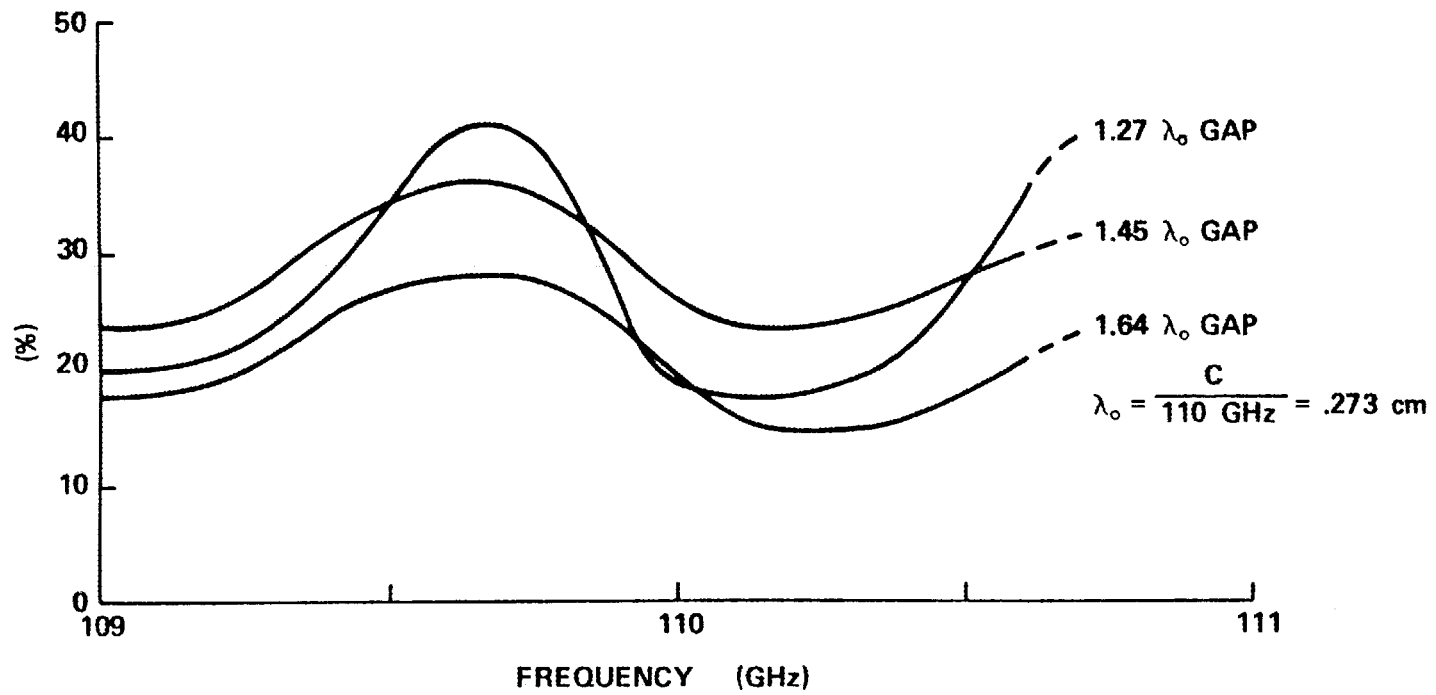


FIGURE 14. TRANSMISSION OF TE_{11} MODE THROUGH ANODE LOAD vs LOAD GAP & FREQUENCY

frequency. A 1.27λ gap provides about 7 dB of loss at 110 GHz. These results are encouraging, and mechanical design of a scaled version of this load cavity is underway for the 60 GHz tube.

2. Effective Interaction Cavity Length

We have used the reactive loading properties of a dielectric bead to investigate the rf field structure in the interaction circuit. The dielectric bead affects the overmoded cavity transmission resonance signal in two ways. There is the familiar dielectric detuning of the resonance frequency f_0 by some frequency shift $\Delta f \sim E_0^2(Z)$. A second effect dominates when the bead is large (i.e., when (bead size) \div (cavity size) $\ll 1$ is not satisfied). In this case the bead imposes boundary conditions which couple the cavity fields to propagating (non-evanescent) waveguide modes. This diminishes the external Q of the cavity from the values, Q_L , measured when the bead is absent. The resulting reduced cavity Q_{EXT} is a function of the axial bead position z . By a simple argument, one can show that the fractional change in Q_{EXT} is related to the cavity field amplitude according to: $(1 - Q_{EXT}(z)/Q_L) \sim E_0^2(Z)$. This expression is valid only when $Z \leq L$ is satisfied. For $Z \geq L$, the bead partially reflects the cavity output signal. In this region, while the data provide no exact information on electric field amplitudes, local maxima in $Q_{EXT}(z)$ are observed at axial positions where the electric field is at a null.

An experiment was performed to determine the rf field structure within the interaction cavity and the nearby output waveguide structure. A small (0.13 cm x 0.13 cm) cylindrical dielectric bead was drawn through the 110 GHz TE_{02} cavity (cavity radius = 0.31 cm) on a nylon thread along a line parallel to the axis of symmetry with a radial displacement corresponding to the position of the first electric field maximum in the cavity. The cavity was excited in the TE_{02} mode and the peak height of the transmission resonance signal, which is roughly proportional to the cavity Q_{EXT} , was observed as a function of bead position. A typical set of data are shown in Figure 15. The cavity contains a one-half wavelength electric field variation which extends slightly beyond the cavity structure toward the output waveguide. From there on toward the collector, the guide wavelength

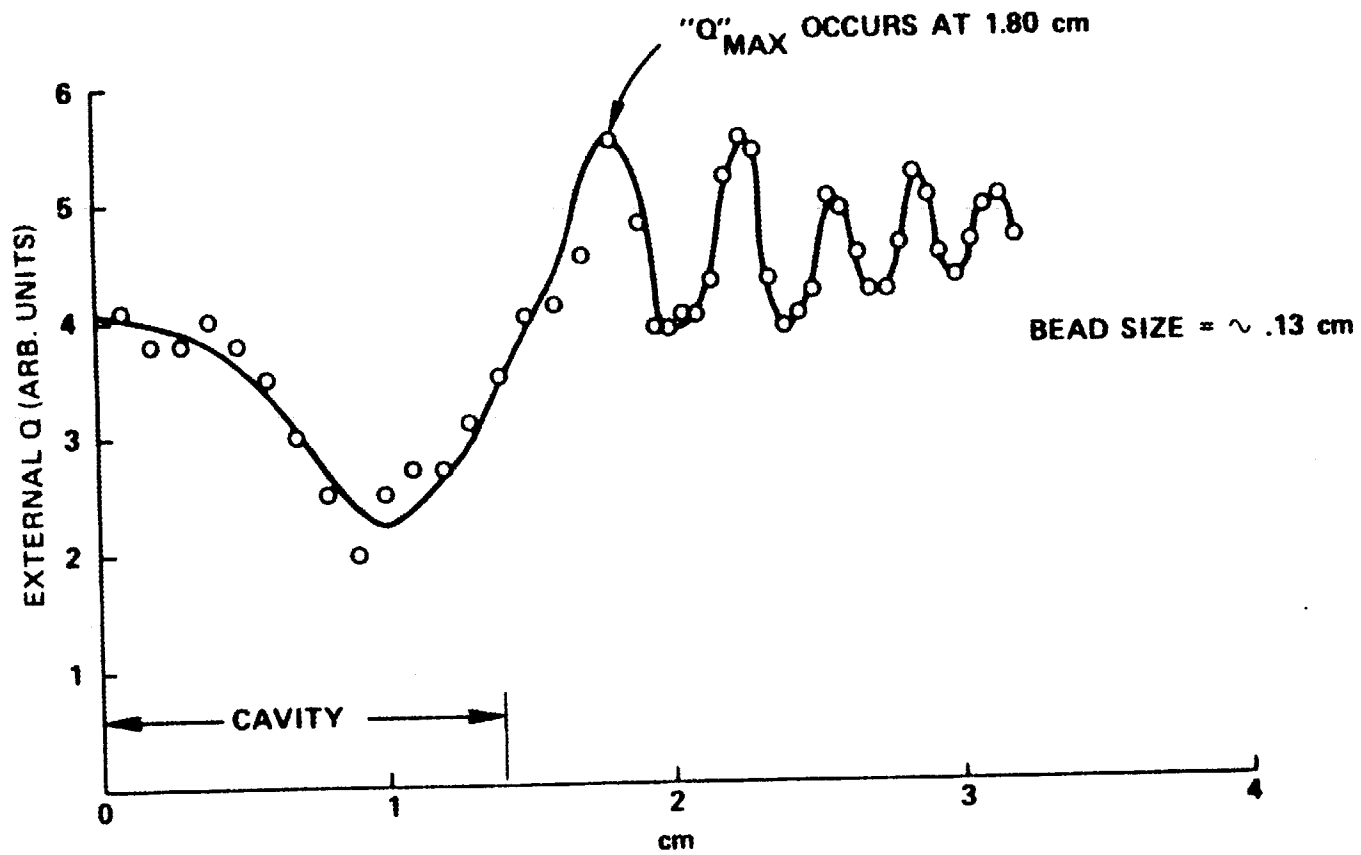


FIGURE 15. EFFECTIVE INTERACTION CAVITY LENGTH

of the rf field decreases, as seen by the decreasing separation between the local maxima in the data. The effective length of the cavity, for lack of a better definition, is therefore the distance between the first two local maxima: in this case 1.8 cm or about 6.6λ .

C. Output Window

The microwave designs for fluorocarbon liquid face cooled double disc alumina and beryllia windows were completed. The long lead time alumina and beryllia discs have been received. Mechanical design of the remaining parts was terminated with the redirection to 60 GHz.

• IV. WATERLOADS, POWER SAMPLERS AND ARC DETECTORS

Piece parts for the waterload have been received. Construction will be completed in time for the first tube test.

Piece parts for the 110 GHz power sampler and arc detector have been received. Assembly has been postponed.

V. PROGRAM SCHEDULE AND PLANS

A schedule for the 60 GHz gyrotron development program is shown in Figure 16.

During the next quarter the electron gun, superconducting solenoid magnet, output/collector and output window designs will be completed. Because of the redirection in frequency, borrowed equipment will be used for cold test measurements until the arrival of our own.

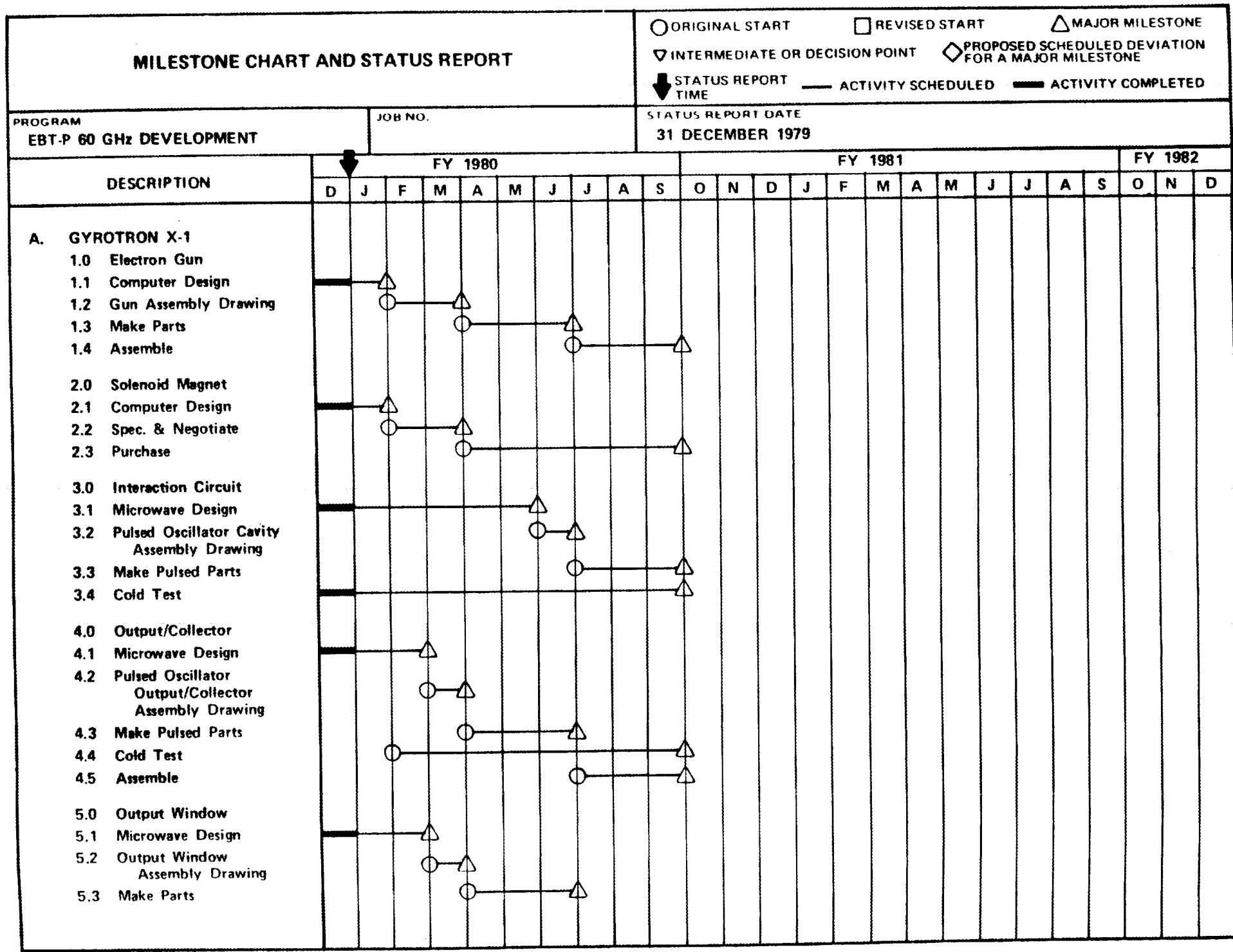


FIGURE 16. MILESTONE CHART

28

MILESTONE CHART AND STATUS REPORT

○ ORIGINAL START □ REVISED START △ MAJOR MILESTONE
 ▽ INTERMEDIATE OR DECISION POINT ◇ PROPOSED SCHEDULED DEVIATION FOR A MAJOR MILESTONE
 ↓ STATUS REPORT TIME — ACTIVITY SCHEDULED — ACTIVITY COMPLETED

PROGRAM
EBT-P 60 GHz DEVELOPMENT

JOB NO.

STATUS REPORT DATE
31 DECEMBER 1979

DESCRIPTION	FY 1980					FY 1981					FY 1982													
	J	A	S	O	N	D	J	F	M	A	M	J	J	A	S	O	N	D	J	F	M	A	M	J
E. GYROTRON 100 ms 2																								
1.0 Make Parts	○	—	—	—	△																			
1.1 Assemble				○	—	—	—	—	△															
1.2 Test							○	—	—	—	△													
1.3 Modify & Reassemble I								○	—	—	—	△												
1.4 Retest I											○	—	—	△										
1.5 Modify & Reassemble II												○	—	—	—	△								
1.6 Retest II													○	—	—	△								
F. GYROTRON 30 s 1																								
1.0 Oscillator Cavity Assembly Drawing								○	—	—	△													
1.1 Output/Collector Assembly Drawing								○	—	—	△													
1.2 Final Assembly Drawing									○	—	—	△												
2.0 Make Parts										○	—	—	—	△										
2.1 Assemble													○	—	—	—	△							
2.2 Test														○	—	—	△							
2.3 Modify & Reassemble I															○	—	—	△						
2.4 Retest I																○	—	—	△					
2.5 Modify & Reassemble II																	○	—	—	△				
2.6 Retest II																		○	—	—	△			

30

MILESTONE CHART AND STATUS REPORT

○ ORIGINAL START □ REVISED START △ MAJOR MILESTONE
 ▽ INTERMEDIATE OR DECISION POINT ◇ PROPOSED SCHEDULED DEVIATION FOR A MAJOR MILESTONE
 ↓ STATUS REPORT TIME — ACTIVITY SCHEDULED — ACTIVITY COMPLETED

PROGRAM
EBT-P 60 GHz DEVELOPMENT

JOB NO.

STATUS REPORT DATE
31 DECEMBER 1979

DESCRIPTION	FY 1981						FY 1982												FY 1983						
	A	M	J	J	A	S	O	N	D	J	F	M	A	M	J	J	A	S	O	N	D.	J	F	M	
G. GYROTRON 30 s 2																									
1.0 Make Parts																									
1.1 Assemble																									
1.2 Test																									
1.3 Modify & Reassemble I																									
1.4 Retest I																									
1.5 Modify & Reassemble II																									
1.6 Retest II																									
H. GYROTRON CW 1																									
1.0 Make Parts																									
1.1 Assemble																									
1.2 Test																									
1.3 Modify & Reassemble I																									
1.4 Retest I																									
1.5 Modify & Reassemble II																									
1.6 Retest II																									
I. 60 GHz COMPONENTS																									
1.0 Build CW Load																									
2.0 Build Deliverable Pulse Load																									
3.0 Build Deliverable Power Sampler Arc Detector																									
4.0 Build Deliverable CW Load																									

31

MILESTONE CHART AND STATUS REPORT

ORIGINAL START REVISED START MAJOR MILESTONE
 INTERMEDIATE OR DECISION POINT PROPOSED SCHEDULED DEVIATION FOR A MAJOR MILESTONE
 STATUS REPORT TIME — ACTIVITY SCHEDULED — ACTIVITY COMPLETED

PROGRAM
EBT-P 60 GHz DEVELOPMENT

JOB NO.

STATUS REPORT DATE
31 DECEMBER 1979

DESCRIPTION	FY 1982												FY 1983								FY 1984				
	D	J	F	M	A	M	J	J	A	S	O	N	D	J	F	M	A	M	J	J	A	S	E	N	D
J. GYROTRON CW 2																									
1.0 Make Parts																									
1.1 Assemble																									
1.2 Test																									
1.3 Modify & Reassemble I																									
1.4 Retest I																									
1.5 Modify & Reassemble II																									
1.6 Retest II																									

32

VI. REFERENCES

1. H.R. Jory, E.L. Lien, and R.S. Symons, Final Report, "Millimeter Wave Study Program," Oak Ridge National Laboratory Order No. Y12 11Y-49438V, November 1975.
2. D.V. Kisel, G.S. Korablev, V.G. Navel'yev, M.I. Petelin and Sh. E. Tsimring, "An Experimental Study of a Gyrotron, Operating at the Second Harmonic of the Cyclotron Frequency, with Optimized Distribution of the High Frequency Field", Radio Engineering and Electronic Physics, Vol. 19, No. 4, 95-100, 1974.
3. S. Hegji, H. Jory, and J. Shively, "Development Program for a 200 KW CW, 28 GHz Gyroklystron Quarterly Report No. 6", Union Carbide Contract No. 53X01617C, Varian Associates, Inc., July through September 1977.
4. H. Jory, S. Evans, S. Hegji, J. Shively, R. Symons, and N. Taylor, "Development Program for a 200 KW, CW, 28 GHz Gyroklystron quarterly report No. 9", Union Carbide Corporation contract No. W-7405-eng-26, ORNL Sub-01617/9, Varian Associates, Inc., April through June 1978.
5. V.A. Flyagin et al, "The Gyrotron", IEEE Trans. MTT-25, No. 6 pp. 522-527, June 1977.
6. F. Friedlander, E. Galli, H. Jory, F. Kinney, K. Miller, J. Shively and R. Symons, "Development Program for a 200 kw CW 28 GHz Gyroklystron quarterly report No. 1", Union Carbide Corporation Contract No. 53X01617C, Varian Associates, Inc., July 1976.
7. F. Friedlander, E. Galli, H. Jory, K. Miller, J. Shively, and R. Symons, "Development Program for a 200 kw CW 28 GHz Gyroklystron quarterly report No. 2, "Union Carbide Corporation Contract No. 53X01617C, Varian Associates, Inc., October 1976.

ORNL/SUB-21453C
2/15/80

INTERNAL DISTRIBUTION

- | | |
|-----------------------|--|
| 1. L. A. Berry | 16. G. F. Pierce |
| 2. A. L. Boch | 17. T. L. White |
| 3. J. L. Burke | 18-19. Laboratory Records Department |
| 4. R. J. Colchin | 20. Laboratory Records, ORNL-RC |
| 5-8. H. O. Eason | 21. Y-12 Document Reference Section |
| 9. O. C. Eldridge | 22-23. Central Research Library |
| 10. R. P. Jernigan | 24. Fusion Energy Division Library |
| 11-13. C. M. Loring | 25. Fusion Energy Division Communications Center |
| 14. H. C. McCurdy | 26. ORNL Patent Office |
| 15. O. B. Morgan, Jr. | |

EXTERNAL DISTRIBUTION

27. K. W. Arnold, Hughes Aircraft Company, Electron Dynamics Division, 3100 W. Lomita Blvd., Torrance, CA 90509
28. R. A. Dandl, 1122 Calle De Los Serranos, San Marcos, CA 92069
29. A. N. Dellis, Culham Laboratory, Abingdon, Oxon, England, OX143DB
30. W. P. Ernst, Princeton University, Plasma Physics Laboratory, P.O. Box 451, Princeton, NJ 08540
31. W. Friz, AFAL/DHM, Wright Patterson AFB, OH 45433
32. T. Godlove, Particle Beam Program, Office of Inertial Fusion, Department of Energy, Mail Stop C-404, Washington, DC 20545
33. V. L. Granatstein, Naval Research Laboratory, Code 6740, Washington, DC 20375
34. G. M. Haas, Component Development Branch, Office of Fusion Energy (ETM), Department of Energy, Mail Stop G-234, Washington, DC 20545
35. J. L. Hirshfield, Department of Engineering and Applied Science, Mason Laboratory, 9 Hillhouse Avenue, Yale University, New Haven, CT 06520
36. H. Ikegami, Institute of Plasma Physics, Nagoya University, Nagoya 464, Japan
37. J. V. Lebacqz, Stanford Linear Accelerator Center, P.O. Box 4349, Stanford, CA 94305
38. K. G. Moses, TRW Defense & Space Systems, 1 Space Park, Bldg. R-1, Redondo Beach, CA 90278
39. M. R. Murphy, Office of Fusion Energy (ETM), Department of Energy, Mail Stop G-234, Washington, DC 20545
40. V. B. Napper, Three Dunwoody Park, Suite 112, Atlanta, GA 30341
41. B. H. Quon, TRW Defense & Space Systems, 1 Space Park, Bldg. R-1, Redondo Beach, CA 90278
42. M. E. Read, Naval Research Laboratory, Code 6740, Washington, DC 20375
43. D. B. Rensen, General Atomic Company, P.O. Box 81608, San Diego, CA 92138
44. B. Stallard, Lawrence Livermore Laboratory, University of California, L-437, P.O. Box 806, Livermore, CA 94550
45. H. S. Staten, Office of Fusion Energy (ETM), Department of Energy, Mail Stop G-234, Washington, DC 20545
46. P. Tellerico, AT-1, Accelerator Technology Division, Los Alamos Scientific Laboratory, Mail Stop 817, P.O. Box 1663, Los Alamos, NM 87545
47. R. J. Temkin, National Magnet Laboratory, Massachusetts Institute of Technology, Cambridge, MA 02139
48. A. Trivelpiece, Science Applications, Inc., 1200 Prospect Street, P.O. Box 2351, LaJolla, CA 92038

INTERNAL DISTRIBUTION (continued)

ORNL/SUB-21453C
2/15/80

49. Director, U.S. Army Ballistic Missile Defense Advance Technology Center, Attn.: D. Schenk,
ATC-R, P.O. Box 1500 Huntsville, AL 35807
- 50-51. Department of Energy Technical Information Center, Oak Ridge, TN 37830
52. RADC/OCTP, GRIFFISS AFB, NY 13441

VARIAN DISTRIBUTION

- 51. R. Berry
- 52. C. Conner
- 53. S. Evans
- 54. P. Ferguson
- 55. J. Jacobs
- 56. H. Jory
- 57. J. Moran
- 58. W. Sayer
- 59-68. J. Shively
- 69. A. Staprans
- 70. D. Stone
- 71. R. Symons
- 72. G. Thomas
- 73. G. Wendell
- 74-75. R. West